The magnetic field dependent dynamic properties of magnetorheological elastomers based on hard magnetic particles

2017 Smart Mater. Struct. 26 075012

(http://iopscience.iop.org/0964-1726/26/7/075012)

IOP Publishing Smart Materials and Structures
Smart Mater. Struct. **26** (2017) 075012 (9pp) https://doi.org/10.1088/1361-665X/aa7396

The magnetic field dependent dynamic properties of magnetorheological elastomers based on hard magnetic particles

Qianqian Wen, Yu Wang and Xinglong Gong

CAS Key Laboratory of Mechanical Behavior and Design of Materials, Department of Modern Mechanics, University of Science and Technology of China, Hefei 230027, People's Republic of China

E-mail: gongxl@ustc.edu.cn

Received 23 November 2016, revised 9 May 2017
Accepted for publication 17 May 2017
Published 14 June 2017

Abstract

In this study, novel magnetorheological elastomers based on hard magnetic particles (H-MREs) were developed and the magnetic field dependent dynamic properties of the H-MREs were further investigated. The storage modulus of H-MREs could not only be increased by increasing magnetic field but also be decreased by the increasing magnetic field of opposite orientation. For the anisotropic H-MREs with 80 wt% NdFeB particles, the field-induced increasing and decreasing modulus was 426 kPa and 118 kPa respectively. Moreover, the dynamic performances of H-MREs significantly depended on the pre-structure magnetic field, magnetizing field and test magnetic field. The H-MREs were initially magnetized and formed the chain-like microstructure by the pre-structure magnetic field. The field-induced increasing and decreasing modulus of H-MREs both raised with increasing of the magnetizing field. When the magnetizing field increased from 400 to 1200 kA m^{-1}, the field induced decreasing modulus of the 80 wt% isotropic H-MREs raised from 3 to 47 kPa. The magnetic field dependent curves of H-MREs' storage modulus were asymmetric if the magnetizing field was higher than the test magnetic field. Based on the dipolar model of MREs and magnetic properties of hard magnetic material, a reasonable explanation was proposed to understand the H-MREs' field dependent mechanical behaviors.

Keywords: magnetorheological elastomer, hard magnetic particles, negative stiffness, dynamic properties

(Some figures may appear in colour only in the online journal)

1. Introduction

Magnetorheological Elastomers (MREs) are a kind of novel smart material with rheological properties which can be controlled rapidly, continuously and reversibly by external magnetic fields [1–4]. Because of these unique properties, MREs have attracted increasing attention and gained broad application. With variable stiffness and damping under magnetic field, MREs are broadly applied in smart devices such as vibration absorbers [5–10], vibration isolators [11–14] and adaptive base isolators [15–17].

MREs are mainly based on soft magnetic particles (S-MREs) and the modulus of S-MREs could only increase with increasing of the magnetic field. This characteristic limits their application in MREs isolator, because it is required to achieve 'negative stiffness' for low-frequency vibrations. For a traditional S-MREs isolator, the electromagnet must always be turned on to provide an initial magnetic field to the S-MREs elements, and then the stiffness could be decreased by decreasing the initial current. It is costly and dangerous due to the power constantly consumed and the heat produced by the electromagnetic coil. Therefore, novel negative

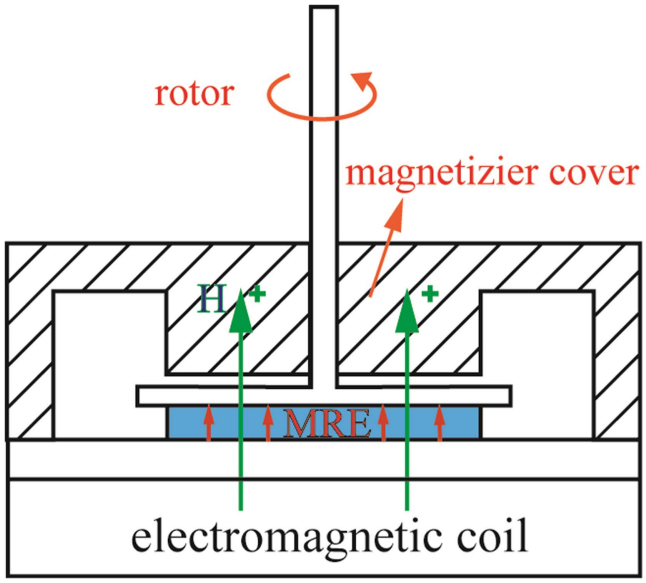

Figure 1. Schematic diagram of the Physica MCR 301 test system.

stiffness MR materials without applying initial magnetic field are urgently required.

Recently, a new type of MREs with hard magnetic particles (H-MREs) embedded within the elastomer was developed. The studies on the actuation abilities [18, 19] and viscoelastic properties [20–24] of H-MREs have been performed. Stepanov *et al* [20, 22] investigated the viscoelastic behavior of the H-MREs and found the modulus could be changed in two ways (to increase and to decrease) on applying a field in opposite directions. Yu *et al* [24] reported the dynamic mechanical responses of the H-MREs to a symmetrical circle magnetic field and found it had the ability of bi-directional magnetic-control modulus. Therefore H-MREs offered the potential to overcome the shortcomings in the traditional S-MREs isolator.

The magnetic field dependent property was one of the most important properties of MREs. However, most of the previous studies on H-MREs were mainly focused on the performance under a single magnetic field loading mode, which limited the fully understanding of dynamic performance of the H-MREs. The magnetic properties of H-MREs are seriously affected by the loading history of magnetic fields, so the corresponding dynamic mechanical performance of H-MREs under external magnetic fields would be much more complex than that of S-MREs. To this end, it is important to comprehensively investigate the performance of H-MREs under different magnetic field loading modes for purpose of better understanding of the H-MREs' mechanism, which is necessary for their practical applications.

In this paper, the dynamic performances of isotropic and anisotropic H-MREs under magnetic field were investigated. The influence of the pre-structure magnetic field, magnetizing field, and test magnetic field on dynamic properties of the H-MREs was also investigated. A possible mechanism based on the quasi-static dipolar model was proposed to explain the mechanical behavior of the H-MREs under external magnetic fields.

2. Experiments section

2.1. Sample preparation

The raw materials included three basic components: unmagnetized NdFeB particles (with a wide size distribution (1–100 μm), provided by Guangzhou Nuode Transmission Parts Co. Ltd, China), Polydimethylsiloxane (PDMS) and curing agent (Sylard 184, purchased from Dow Corning GmbH, USA). The fabrication of H-MREs consisted of three major steps: firstly, the three basic components, NdFeB particles, PDMS and curing agent, were mixed thoroughly into a homogenous mixture in appropriate proportions. Secondly, the mixture was put into vacuum chamber for 15 min in order to remove internal air bubbles. Finally, the mixture was placed into an aluminum mold and cured at 80 °C for 30 min without the presence of a magnetic field for isotropic H-MREs or under a pre-structure magnetic field for anisotropic H-MREs. In this study, all the anisotropic H-MREs were cured and initially magnetized under the same pre-structure magnetic field of 1200 kA m^{-1} for 30 min. Six kinds of isotropic and anisotropic H-MREs with NdFeB particle content of 40 wt%, 60 wt% and 80 wt% (correspond to 7.7 vol%, 15.8 vol% and 33.4 vol% respectively) were prepared. The six kinds of samples were named as iso-40, iso-60, iso-80, ani-40, ani-60 and ani-80 respectively. For comparison, the elastomer matrix without any particles was also prepared.

2.2. Characterization of the magnetic and dynamic properties

The magnetic properties of the particles were measured by Hysteresis Measurement of Soft and Hard Magnetic Materials (HyMDC Metis, Leuven, Belgium). The test magnetic field was set as 400, 600, 800, 1000 and 1200 kA m^{-1} respectively to test the particles' hysteresis under different magnetic field.

The dynamic properties of the H-MREs were measured by rheometer (Physica MCR 301, Anton Paar Co., Austria). As shown in figure 1, the test sample (diameter 20 mm and thickness 1 mm) was placed between the rotating disk and the base. The test magnetic field, controlled by the current applied to the electromagnetic coil, was parallel to the thickness of the sample. The magnetic field of rheometer could be controlled in two orientations. The orientation of the magnetic field was defined as positive (shown as green arrows in figure 1) when it was the same with the inner particles' initial residual magnetization (shown as red arrows in figure 1). 20 N of pre-pressure was applied on the sample to prevent it from sliding on the base. The tests were in the oscillating mode and all samples were tested at strain amplitude of 0.1%, frequency of 5 Hz, temperature of 25 °C and measuring interval of 1 s.

3. Results and discussions

Figure 2 showed the hysteresis loops of the pure NdFeB particles under different test magnetic field. The NdFeB particles were unmagnetized before the test, so figure 2 could

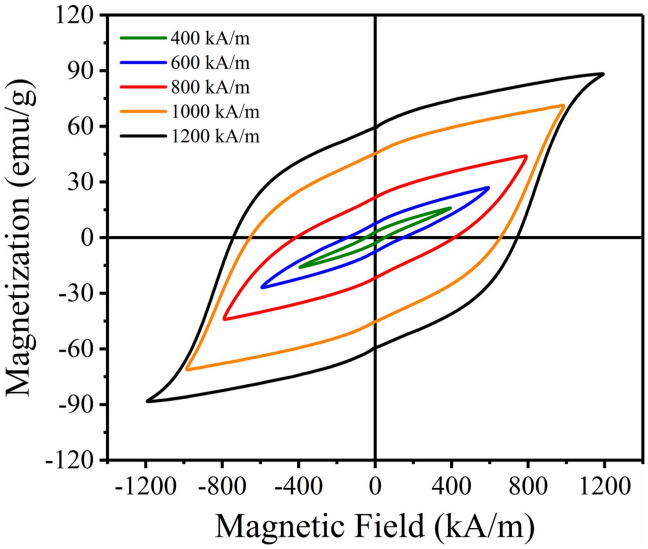

Figure 2. The hysteresis loops (magnetization versus magnetic field) of pure NdFeB particles under different magnetic field.

be regarded as the hysteresis loops of the pure unmagnetized NdFeB particles under different magnetizing field. It could be seen that both the residual magnetization and coercive force of NdFeB particles increased with the increasing of the magnetizing field. When the magnetizing field was 400 kA m^{-1}, residual magnetization and coercive force was only 2.92 emu g^{-1} and 49.7 kA m^{-1}. When the magnetizing field was 1200 kA m^{-1}, residual magnetization and coercive force increased to 49.37 emu g^{-1} and 742.6 kA m^{-1}. Figure 2 showed the typical magnetic behavior of the hard magnetic materials, which indicated that the magnetizing field would play an important role in the dynamic properties of the H-MREs.

Figure 3 showed the microstructures of the iso-60 and ani-60 H-MREs. Obviously, the internal NdFeB particles had a wide size distribution and irregular shapes. The NdFeB particles were unmagnetized before sample preparation. The isotropic samples were prepared in the absence of a pre-structure magnetic field, therefore the particles were randomly distributed without the any magnetic interaction (figure 3(a)). In contrast, the anisotropic samples were prepared under the pre-structure field and the internal particles were magnetized during the preparation. The magnetic interaction between the particles forced them to form chain-like structure along the direction of the pre-structure field (figure 3(b)).

Figure 4 showed the magnetic field dependent storage modulus of all the isotropic and anisotropic H-MREs. The samples were tested under symmetrical cyclic magnetic field of 800 kA m^{-1}. We defined that the orientation of the test magnetic field was negative when it was opposite to the inner particles' initial residual magnetization as shown in figure 1. The cyclic magnetic field first increased in the negative direction from 0 to −800 kA m^{-1}. The measuring interval was 1 s and the magnetic field cycle time was 80 s.

Taking the ani-80 sample as an example, under the cyclic magnetic field, its storage modulus started to decrease from initial point 'S' to the left minimum point 'A', and then began to increase to the left maximum point 'B'. The overall change trends of ani-80 sample's storage modulus were shown as the curve 'S-A-B-C-D-S'. For all the six samples, their change trends of the storage modulus were similar. When the magnetic field (in positive or negative orientation) decreased from maximum to zero and started to increase in the opposite direction, the modulus firstly decreased and then increased.

Particularly, the curve 'D-S-A' was one of the most interesting dynamic properties of the H-MREs, which showed the H-MREs not only had 'positive modulus' (increased with increasing of magnetic field) but also 'negative modulus' (decreased with increasing of magnetic field). The positive and negative modulus demonstrated the modulus of the H-MREs could be controlled in two ways (increase and decrease) by varying orientation of the magnetic field. More importantly, the start point 'S' indicated that the positive and negative modulus of H-MREs was achieved without applying the initial field. This extraordinary property could provide a possible way to solve the problem in the S-MREs isolator that it must provide initial field to support 'negative stiffness'. The negative modulus ($\Delta G'_{-}$) of the ani-80 sample was equal to the initial storage modulus (G'_{int}) at point 'S' minus the minimum storage modulus (G'_{min}) at point 'A'. The positive modulus ($\Delta G'_{+}$) of the ani-80 sample was equal to the maximum storage modulus (G'_{max}) at point 'D' minus the initial storage modulus (G'_{int}) at point 'S'. Detail information of all the H-MREs' moduli were listed in table 1.

It was found that the content and structure of particles had great influence on the storage modulus of H-MREs. The H-MREs with higher particles content exhibited the higher overall storage modulus. For example, the G'_{int} of iso-80 sample was 1225 kPa while the G'_{int} of iso-40 sample was only 148 kPa. The field-induced positive and negative modulus of anisotropic H-MRESs was much higher than the isotropic one with the same content. The influence of particles' content and structure on the storage modulus of H-MREs was similar to S-MREs. This was attributed that both S-MREs and H-MREs were magnetic particles reinforced composites and had the similar microstructures.

Meanwhile, it was worth noting from figure 4 that the variation of all the isotropic H-MREs' storage modulus under cyclic magnetic field were symmetric while that of anisotropic H-MREs were very asymmetric. The asymmetry was reflected at two aspects. One was the difference between the left maximum storage modulus and right maximum storage modulus. The other was difference between the magnetic field strength of left minimum storage modulus and magnetic field strength of right minimum storage modulus. Taking the ani-80 sample as an example, the magnetic field strength at point 'A' (H_{A}) was higher than magnetic field strength at point 'C' (H_{C}), and the storage modulus at point B (G_{B}') was smaller than the storage modulus at point D (G_{D}'). However this asymmetry has not been reported in the previous studies on S-MREs. The previous works often focused on their dynamic properties under unidirectional increasing magnetic field while the studies on the dynamic properties of S-MREs under cyclic magnetic field were few reported [1–4]. The different inner particles in H-MREs and S-MREs resulted in the

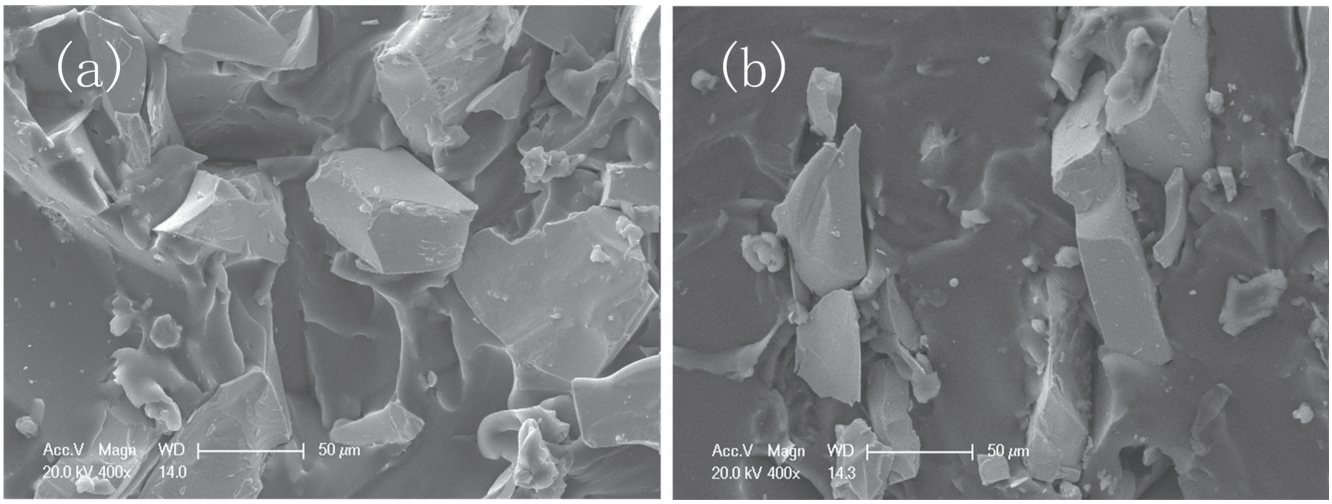

Figure 3. SEM images of (a) iso-60; (b) ani-60 H-MREs.

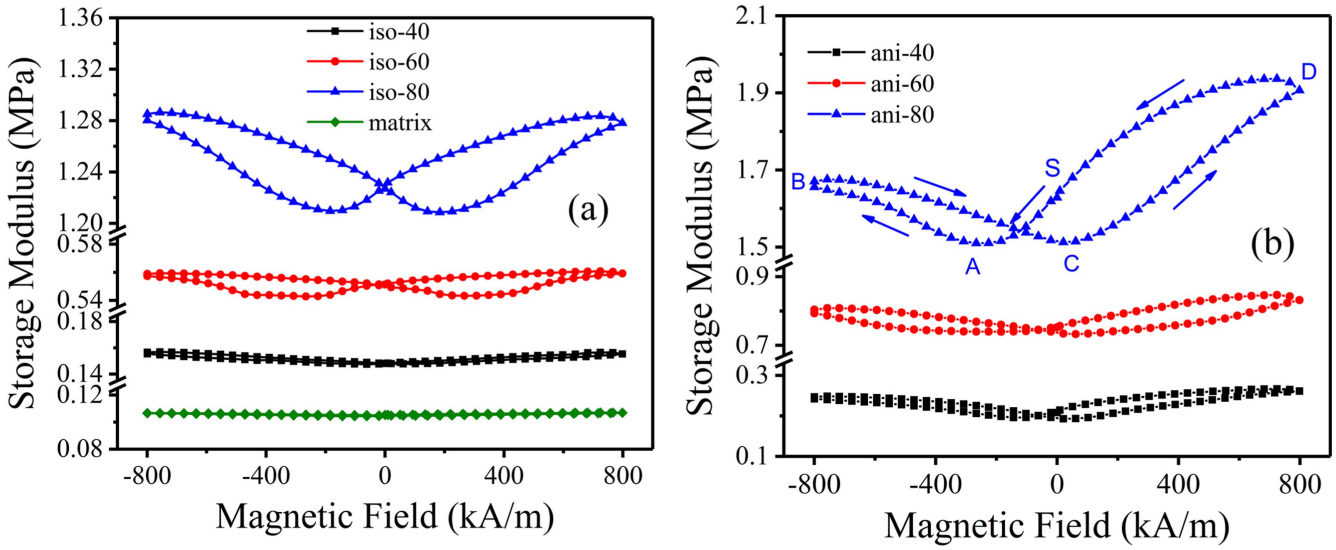

Figure 4. The storage modulus versus magnetic field for (a) isotropic and (b) anisotropic H-MREs.

Table 1. The G'_{int}, G'_{min}, G'_{max}, $\Delta G'_{-}$ and $\Delta G'_{+}$ of H-MREs samples.

Samples	Initial storage modulus G'_{int} (kPa)	Minimum storage modulus G'_{min} (kPa)	Maximum storage modulus G'_{max} (kPa)	Negative modulus $\Delta G'_{-} = G'_{int} - G'_{min}$ (kPa)	Positive modulus $\Delta G'_{+} = G'_{max} - G'_{int}$ (kPa)
iso-40	148	147	155	1	7
iso-60	552	543	561	9	9
iso-80	1225	1210	1284	15	59
ani-40	209	196	267	7	58
ani-60	753	540	847	13	107
ani-80	1628	1510	1936	118	426

different dynamic behaviors under changing external magnetic field. For comparison, the hysteresis loops of soft magnetic carbonyl iron (CI) particles (type CN, with an average diameter of 6 μm, provided by BASF Co., Germany) and the dynamic properties of S-MERs based on CI particles were also tested.

Figure 5 showed the hysteresis loops of the pure CI particles under different magnetizing field. The residual magnetization and coercive force of the CI particles were much smaller than that of NdFeB under the same magnetizing field. For example, the residual magnetization and coercive force of NdFeB particles with magnetizing field of 1000 kA m^{-1} were 45.4 emu g^{-1} and

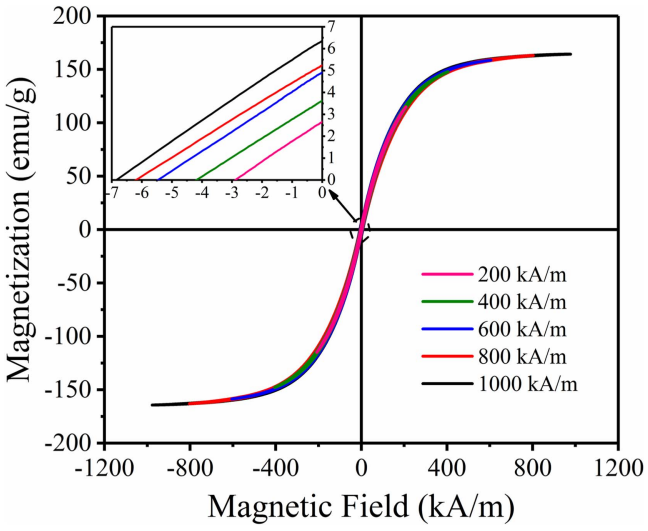

Figure 5. The hysteresis loops (magnetization versus magnetic field) of pure carbonyl iron (CI) particles under different magnetic field.

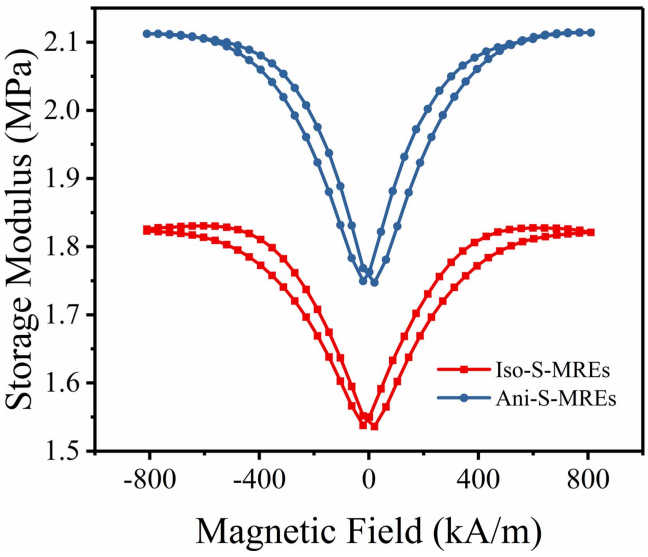

Figure 6. The storage modulus versus magnetic field of the isotropic and anisotropic S-MREs with 80 wt% CI particles.

654.9 kA m^{-1} respectively, while the residual magnetization and coercive force of CI particles with magnetizing field of 1000 kA m^{-1} were 6.3 emu g^{-1} and 7.1 kA m^{-1}.

Figure 6 showed the magnetic field dependent storage modulus of the isotropic and anisotropic S-MREs with 80 wt% CI particles. The preparation of isotropic and anisotropic S-MREs was the same as H-MREs'. No negative modulus and the asymmetry properties were appeared whether for isotropic S-MREs or anisotropic one (figure 6) due to that the residual magnetization of the CI particles was much smaller than NdFeB particles'. The pre-structure magnetic field not only drove the inner particles to form chain-like structure, but also made the H-MREs magnetized at a preliminary stage to obtain residual magnetization [21].

To study the effect of pre-structure field, we designed a control experiment to test the dynamic properties of the iso-80 sample magnetized under the same pre-structure magnetic field

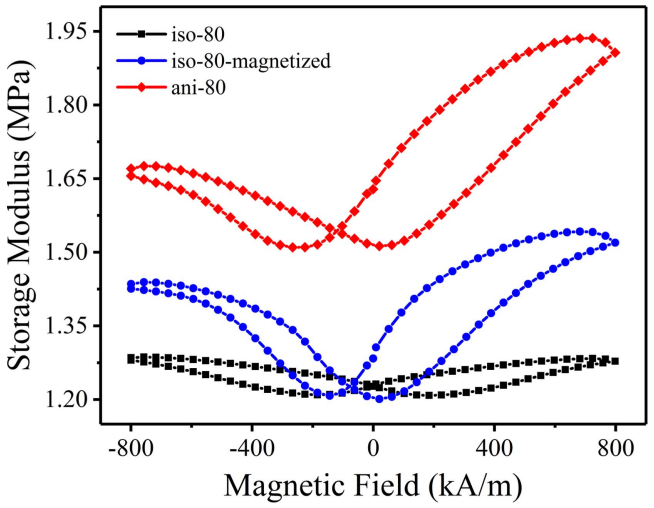

Figure 7. The storage modulus versus magnetic field for iso-80, ani-80 and iso-80 magnetized by the pre-structure field.

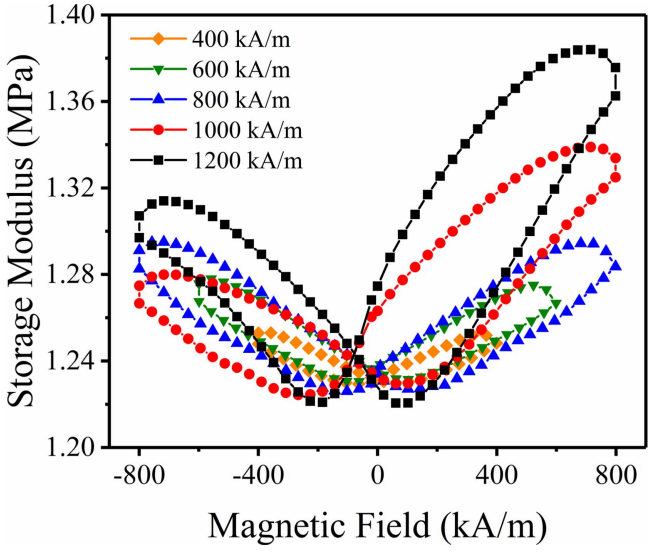

Figure 8. The storage modulus versus magnetic field for iso-80 H-MREs with different magnetizing fields.

of 1200 kA m^{-1}. Figure 7 showed the magnetic field dependent storage moduli of iso-80, ani-80 and iso-80 magnetized by the pre-structure field. It proved that the chain-like structure and residual magnetization exhibited different influence on the dynamic properties. The comparison between 'iso-80-magnetized' and 'ani-80' illustrated that the chain-like structure could improve the overall storage modulus. The comparison between 'iso-80' and 'iso-80-magnetized' indicated that the magnetizing field caused the asymmetric curve. The influence of the chain-like structure on the dynamic performance of H-MREs was the same with that of S-MREs, which was in accordance with the previous studies [25, 26]. However, the unique performance that magnetizing field resulted in the asymmetric field dependent curve of storage modulus, has not been explained yet.

To better understand the effect of the magnetizing field, the dynamic properties of the isotropic H-MREs with different magnetizing fields were investigated. Figure 8 showed the

Table 2. The G'_{int}, G'_{min}, G'_{max}, $\Delta G'_{-}$ and $\Delta G'_{+}$ of iso-80 H-MREs with different magnetizing fields.

Magnetizing field (kA m^{-1})	Initial storage modulus G'_{int} (kPa)	Minimum storage modulus G'_{min} (kPa)	Maximum storage modulus G'_{max} (kPa)	Negative modulus $\Delta G'_{-} = G'_{int} - G'_{min}$ (kPa)	Positive modulus $\Delta G'_{+} = G'_{max} - G'_{int}$ (kPa)
400	1232	1229	1252	3	20
600	1236	1230	1275	4	39
800	1238	1226	1294	12	56
1000	1260	1224	1339	36	79
1200	1268	1221	1384	47	116

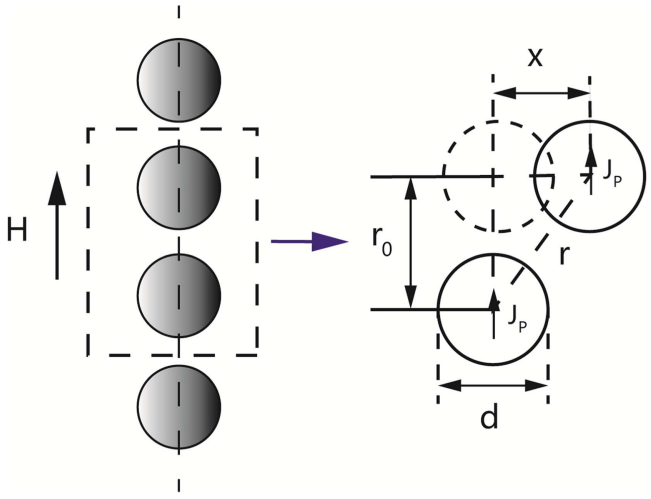

Figure 9. Schematic diagram of dipolar model of the MRE.

magnetic field dependence of the iso-80 samples' storage modulus. The different magnetizing fields were applied on iso-80 for 1 min before the test for preliminary magnetization. The tests were divided into two cases: (1) magnetizing field was equal to amplitudes of the test magnetic field loops; (2) magnetizing field was higher than fixed amplitude of the test magnetic field loops. Taking into account the magnetization of the test magnetic field, the case that magnetizing field was less than amplitudes of the test magnetic field loops was the same to the case 1. As shown in figure 8, the curves of iso-80 samples' storage modulus with magnetizing field of 400, 600, 800 kA m^{-1} were both symmetric while the curves with magnetizing field of 1000, 1200 kA m^{-1} become more and more asymmetric with increasing of magnetizing filed. It indicated that whether the dynamic property curves were symmetric or not was determined by the relationship between magnetizing field and amplitude of test magnetic field. When the magnetizing field was equal to the amplitude of cyclic test magnetic field, the dynamic properties curves was symmetric. When the magnetizing field was higher than the amplitude of test magnetic field loops, the dynamic properties curves appeared asymmetric. The detail information about the G'_{int}, G'_{min}, G'_{max}, $\Delta G'_{-}$ and $\Delta G'_{+}$ of the iso-80 H-MREs sample with different magnetizing fields was listed in table 2. G'_{int}, G'_{max}, $\Delta G'_{-}$ and $\Delta G'_{+}$ increased with increasing of magnetizing field while the G'_{min} changed slightly with the different magnetizing fields. When the magnetizing field raised from 400 to 1200 kA m^{-1}, the G'_{int} increased from 1232 to 1268 kPa while the G'_{min} remained at about 1225 kPa.

In order to understand the above dynamic properties of H-MREs under external magnetic field, a reasonable explanation based on the dipolar model (figure 9) was developed. The model was proposed by Jolly *et al* to explain the modulus change inside of an MR elastomer [1]. According to the model, the field induced storage modulus $\Delta G'$ could be expressed by equation (1):

$$\Delta G' = \frac{\phi {J_P}^2}{2\mu_0\mu_1 h^3} \quad \varepsilon < 0.1, \tag{1}$$

where μ_1 is the relative permeability of the matrix, ϕ is the volume fraction of particles in the composite, h ($=r_0/d$) is an indication of the gap between particles in a chain and J_P is the dipole moment magnitude per unit particle volume. To study the magnetic field dependent properties for single sample, the equation (1) could be expressed as:

$$\Delta G' = \frac{\phi {J_P}^2}{2\mu_0\mu_1 h^3} = K(\phi, \mu_1, h)^* {J_P}^2 \quad \varepsilon < 0.1. \tag{2}$$

Equation (2) showed that once a certain MRE was cured, the volume fraction of particles, the relative permeability of the matrix and the gap between particles were invariable, so the $K(\phi, \mu_1, h)$ was fixed and the change trends of the storage modulus ($\Delta G'$) would be mainly determined by the magnetization (J_P). The larger the magnetization, the stronger the interaction force between particles and the higher the field induced storage modulus. It should be emphasized that both the interaction force and field induced storage modulus were independent of the orientation of the magnetization.

The magnetization of the magnetic material under external field is generally characterized by the hysteresis loops. However, the test of the hysteresis loops requires that initial state of samples is non-magnetized, so the test magnetic field was also as the magnetizing field and the measured hysteresis loop is always symmetric (shown in figure 2). According to equation (2) and the symmetric hysteresis loop, the tendencies of magnetization and the field-induced storage modulus could be expressed by figure 10(a). The tendency of the storage modulus was coincide well with experiment results shown in figure 4(a). If the negative field were initially applied on isotropic H-MREs, H-MREs within the matrix were degaussed at first, so the storage modulus decreased as the curve 's-a' showed. When the negative field continued to increase, the particles started to magnetize at the negative orientation and the storage modulus began to increase as the curve 'a-b' showed. When the negative field decreased from

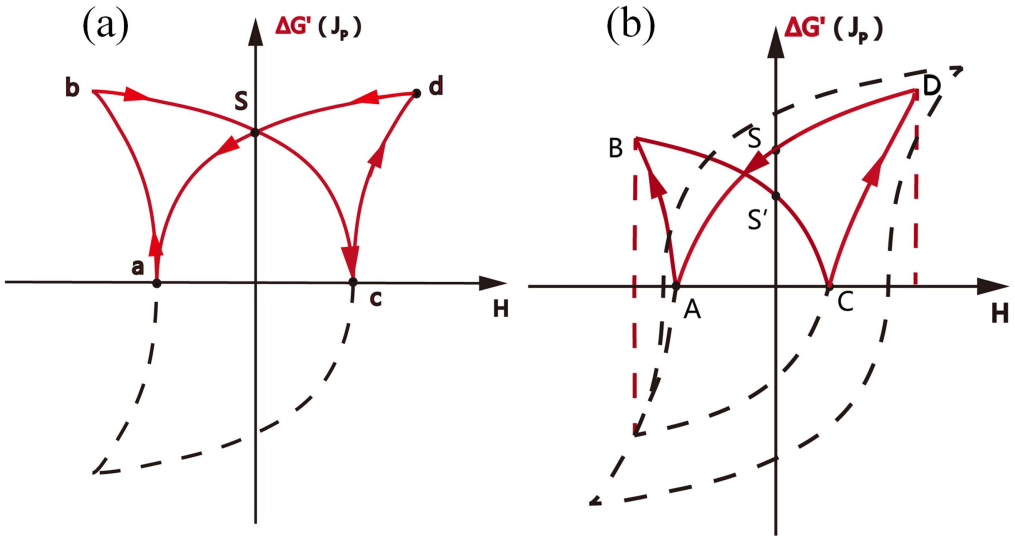

Figure 10. Schematic diagram of the variation trends of (a) symmetric and (b) asymmetric magnetization and storage modulus.

maximum to zero, the magnetization of particles at the negative orientation started to decrease, so the storage modulus decreased as the curve 'b-s' showed. When the field changed at the positive orientation, because of the symmetry of the hysteresis loops, the tendency of the storage modulus was the same to that at negative orientation as the curve 's-c-b-s' showed. Furthermore, it also could be concluded that for a certain H-MREs sample, the negative and positive modulus was determined by the residual magnetization and maximum magnetization. The higher magnetizing field, the larger the residual magnetization and maximum magnetization, and the higher the negative modulus and positive modulus (table 2). Because of the very small residual magnetization of the soft magnetic material (figure 5), there was almost no negative modulus for S-MREs (figure 6).

In the practical application, the hysteresis loops of hard magnetic materials' magnetization under external magnetic field are not always symmetric. When the external magnetic field was smaller than magnetizing field, the hysteresis loops was asymmetry [27]. The schematic diagram of the asymmetric hysteresis loop and corresponding field induced modulus could be sketched in figure 10(b). Clearly, the tendency of theoretical predictions was consistent perfectly with the experiment result (figure 8). As shown in figures 8 and 10, when the magnetizing field was equal to the test magnetic field, the field dependent curves of the storage modulus were symmetric. When the magnetizing field was higher than test magnetic field, the field dependent curves of the storage modulus appeared asymmetric. Furthermore, with increasing difference between magnetizing field and test magnetic field, the field dependent curves of the storage modulus would be more and more asymmetric. In addition, the field dependent curves of anisotropic H-MREs' storage modulus were also asymmetric (figure 4(b)). It was mainly because that the prestructure field of 1200 kA m^{-1} was higher than the test field of 800 kA m^{-1}. It should be noted that no matter the tendencies of storage modulus were symmetric or not, the left minimum storage modulus was always equaled to the right minimum storage modulus (figures 4 and 8). It could be explained by that the corresponding magnetization at the left or right minimum point

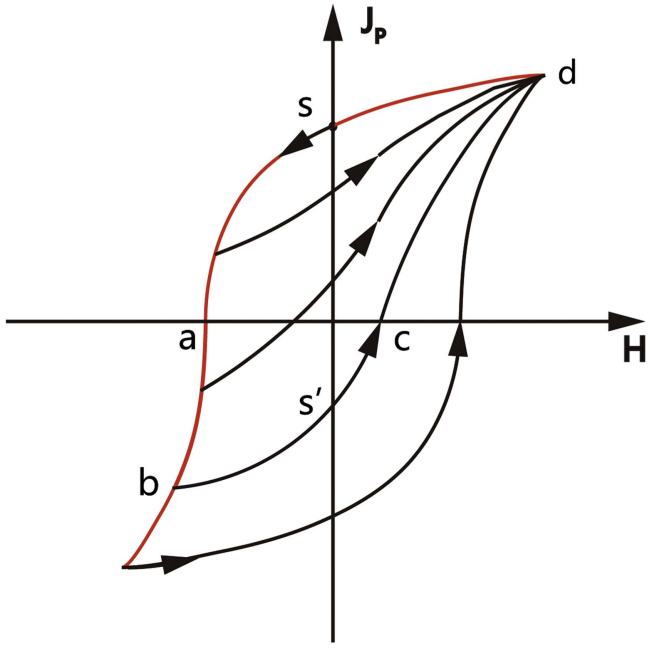

Figure 11. Schematic diagram of the first order reversal curves (FORC).

was both zero just as the point 'a', 'c', 'A' and 'c' showed in figure 10.

To further verify our explanation that the magnetic properties of NdFeB particles played a key role in the tendency of H-MREs' storage modulus under magnetic field, the influence of the test magnetic field on the storage modulus has also been investigated. The hysteresis loop curves where the magnetization reached saturation at negative and positive field extremes were also known as the major loop hysteresis curves, which were the primary means of characterizing ferromagnetism. In addition to major loop hysteresis, the first order reversal curves (FORC, shown as figure 11), where the magnetization saturated at positive field extremum but not saturated at negative field extremum, were the other important

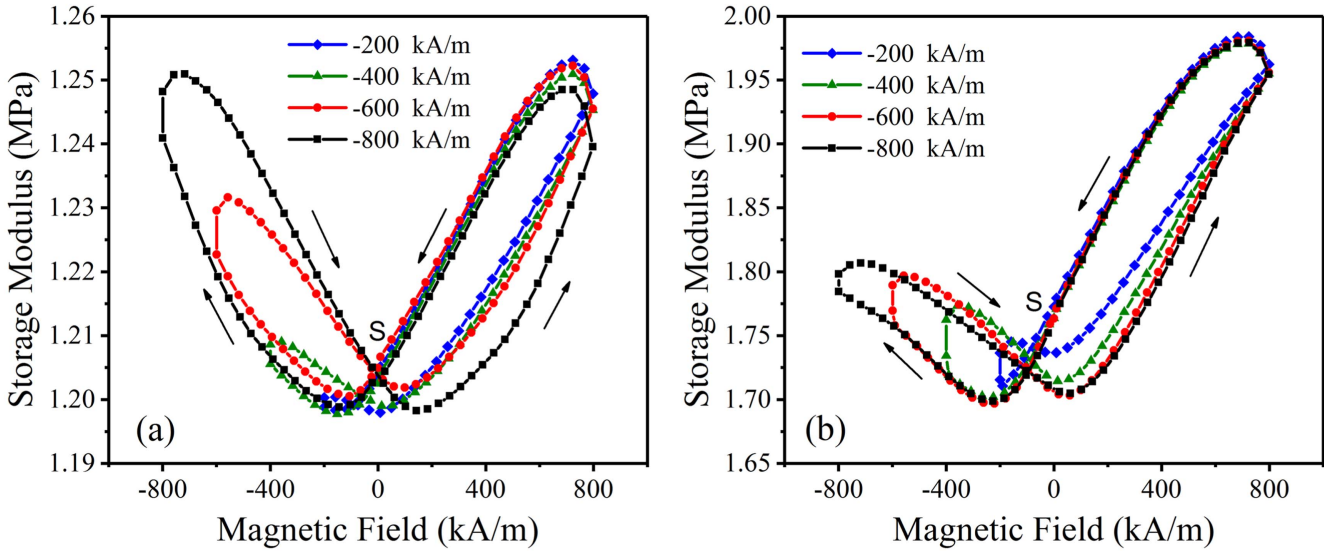

Figure 12. The storage modulus versus magnetic field with different negative extremums of the test magnetic field loops for (a) iso-80 and (b) ani-80 H-MREs.

magnetic properties of the hard magnetic materials [27–31]. Figure 11 showed that if the external magnetic field reversed at the field which was less than extremum, such as at the point 'b', the magnetization would followed the minor loop 'b-s′-d' rather than the initial curve 'b-s-d'. It illustrated that if the hard magnetic materials were applied on negative field and then removed the field, the magnetization of material would change from 's' to 's′'. This irreversible magnetic property of the hard magnetic material would lead to the corresponding irreversible dynamic performance of H-MREs (figure 4). The storage moduli of anisotropic H-MREs at zero magnetic field were not equal. It required a specific loading mode of the external field to make the field dependent performance (especially the negative modulus and positive modulus) of the H-MRE be repeatable.

It's worth noting that all the minor loops in figure 11 would rejoin the major loop at the point 'd' (positive field extremum). The different minor loops had the partial common magnetic characteristic curve as the 'd-s-a' shows. This part of the hysteresis loop determined the positive modulus and negative modulus of H-MREs according to the proposed relationship between the magnetization and storage modulus. Therefore, the positive and negative modulus of the H-MREs would be the same if the external field was applied as the mode of FORC. Here, the field dependence storage moduli of iso-80 and ani-80 samples were tested under different test magnetic field (figure 12). The loading modes of test magnetic field were the same to FORC. The negative field extremums of the test magnetic fields loops were −200, −400, −600 and −800 kA m^{-1} respectively and the positive filed extremums were both 800 kA m^{-1}. It could be seen that both the isotropic and anisotropic samples showed the same positive modulus and negative modulus at the same positive field extremum. It agreed well with the prediction from the FORC of the hard magnetic materials. This characteristic also provided the promise that the H-MREs could have the same positive and negative modulus under different magnetic field loops, which is very important for the practical applications of H-MREs.

4. Conclusions

In this work, a series of isotropic and anisotropic MREs based on H-MREs were prepared and the magnetic field dependent dynamic properties of the H-MREs were investigated. The H-MREs showed not only positive modulus but also negative modulus without applying of the initial magnetic field.

Furthermore, the effect of pre-structure field, magnetizing field and test magnetic field on the storage modulus of H-MREs was investigated. The results showed: (1) the anisotropic H-MREs formed the chain-like structure and were initially magnetized by the pre-structure field; (2) the positive and negative modulus of H-MREs both increased with increasing of the magnetizing field; (3) the relationship between the magnetizing field and test magnetic field would affect the symmetry of H-MREs' dynamic properties' curves. If the magnetizing field was higher than the test magnetic field, the curves of dynamic properties would appear asymmetry.

A possible mechanism based on the dipolar model was proposed to explain magnetic field dependent storage modulus of the H-MREs. The tendencies of the storage modulus by theoretical prediction matched the experimental results well.

Acknowledgments

Financial support from the National Natural Science Foundation of China (Grant No. 11572309) and the Strategic Priority Research Program of the Chinese Academy of Sciences (Grant No. XDB22040502) are gratefully acknowledged. This work was also supported by the Collaborative Innovation Center of Suzhou Nano Science and Technology.

References

[1] Rigbi Z and Jilken L 1983 The response of an elastomer filled with soft ferrite to mechanical and magnetic influences *J. Magn. Magn. Mater.* **37** 267–76

[2] Jolly M R, Carlson J D and Munoz B C 1996 A model of the behaviour of magnetorheological materials *Smart Mater. Struct.* **5** 607–14

[3] Carlson J D and Jolly M R 2000 MR fluid, foam and elastomer devices *Mechatronics* **10** 555–69

[4] Gong X L, Zhang X Z and Zhang P Q 2005 Fabrication and characterization of isotropic magnetorheological elastomers *Polym. Test.* **24** 669–76

[5] Ginder J M, Schlotter W F and Nichols M E 2001 Magnetorheological elastomers in tunable vibration absorbers *Proc. SPIE* **4331** 103–10

[6] Lerner A A and Cunefare K A 2008 Performance of MRE-based vibration absorbers *J. Intell. Mater. Syst. Struct.* **19** 551–63

[7] Xu Z B, Gong X L, Liao G J and Chen X M 2010 An active-damping-compensated magnetorheological elastomer adaptive tuned vibration absorber *J. Intell. Mater. Syst. Struct.* **21** 1039–47

[8] Liao G J, Gong X L, Kang C J and Xuan S H 2011 The design of an active-adaptive tuned vibration absorber based on magnetorheological elastomer and its vibration attenuation performance *Smart Mater. Struct.* **20** 075015

[9] Sinko R, Karnes M, Koo J H, Kim Y K and Kim K S 2013 Design and test of an adaptive vibration absorber based on magnetorheological elastomers and a hybrid electromagnet *J. Intell. Mater. Syst. Struct.* **24** 803–12

[10] Sun S S, Deng H X, Yang J, Li W H, Du H P, Alici G and Nakano M 2015 An adaptive tuned vibration absorber based on multilayered MR elastomers *Smart Mater. Struct.* **24** 045045

[11] Eem S H, Jung H J and Koo J H 2011 Application of MR elastomers for improving seismic protection of base-isolated structures *IEEE Trans. Magn.* **47** 2901–4

[12] Liao G J, Gong X L, Xuan S H, Kang C J and Zong L H 2011 Development of a real-time tunable stiffness and damping vibration isolator based on magnetorheological elastomer *J. Intell. Mater. Syst. Struct.* **23** 25–33

[13] Opie S and Yim W 2011 Design and control of a real-time variable modulus vibration isolator *J. Intell. Mater. Syst. Struct.* **22** 113–25

[14] Kim Y K, Bae H I, Koo J H, Kim K S and Kim S 2012 Note: real time control of a tunable vibration absorber based on magnetorheological elastomer for suppressing tonal vibrations *Rev. Sci. Instrum.* **83** 046108

[15] Li Y C, Li J C, Li W H and Samali B 2013 Development and characterization of a magnetorheological elastomer based adaptive seismic isolator *Smart Mater. Struct.* **22** 035005

[16] Li Y C, Li J C, Tian T F and Li W H 2013 A highly adjustable magnetorheological elastomer base isolator for applications of real-time adaptive control *Smart Mater. Struct.* **22** 095020

[17] Behrooz M, Wang X J and Gordaninejad F 2014 Performance of a new magnetorheological elastomer isolation system *Smart Mater. Struct.* **23** 045014

[18] Koo J H, Dawson A and Jung H J 2012 Characterization of actuation properties of magnetorheological elastomers with embedded hard magnetic particles *J. Intell. Mater. Syst. Struct.* **23** 1049–54

[19] Siegfried P, Koo J H and Pechan M 2014 Torque characterization of functional magnetic polymers using torque magnetometry *Polym. Test.* **37** 6–11

[20] Stepanov G V, Chertovich A V and Kramarenko E Y 2012 Magnetorheological and deformation properties of magnetically controlled elastomers with hard magnetic filler *J. Magn. Magn. Mater.* **324** 3448–51

[21] Borin D Y, Stepanov G V and Odenbach S 2013 Tuning of the tensile modulus of the magnetorheological elastomer with magnetic hard powder *J. Phys.: Conf. Ser.* **412** 012040

[22] Stepanov G V, Borin D Y, Kramarenko E Y, Bogdanov V V, Semerenko D A and Storozhenko P A 2014 Magnetoactive elastomer based on magnetically hard filler: synthesis and study of viscoelastic and damping properties *Polym. Sci. Ser.* A **56** 603–13

[23] Kramarenko E Y, Chertovich A V, Stepanov G V, Semisalova A S, Makarova L A, Perov N S and Khokhlov A R 2015 Magnetic and viscoelastic response of elastomers with hard magnetic filler *Smart Mater. Struct.* **24** 035002

[24] Yu M, Qi S, Fu J and Zhu M 2015 A high-damping magnetorheological elastomer with bi-directional magnetic-control modulus for potential application in seismology *Appl. Phys. Lett.* **107** 111901

[25] Chen L, Gong X L and Li W H 2007 Microstructures and viscoelastic properties of anisotropic magnetorheological elastomers *Smart Mater. Struct.* **16** 2645–50

[26] Kaleta J, Krolewicz M and Lewandowski D 2011 Magnetomechanical properties of anisotropic and isotropic magnetorheological composites with thermoplastic elastomer matrices *Smart Mater. Struct.* **20** 085006

[27] Hauser H 1994 Energetic model of ferromagnetic hysteresis *J. Appl. Phys.* **75** 2584–96

[28] Fulmek P L and Hauser H 1996 Magnetization reversal in an energetic hysteresis model *J. Magn. Magn. Mater.* **160** 35–7

[29] Pike C R, Roberts A P and Verosub K L 1999 Characterizing interactions in fine magnetic particle systems using first order reversal curves *J. Appl. Phys.* **85** 6660–7

[30] Chiriac H, Lupu N, Stoleriu L, Postolache P and Stancu A 2007 Experimental and micromagnetic first-order reversal curves analysis in NdFeB-based bulk 'exchange spring'-type permanent magnets *J. Magn. Magn. Mater.* **316** 177–80

[31] Cao Y, Xu K, Jiang W L, Droubay T, Ramuhalli P, Edwards D, Johnson B R and Mccloy J 2015 Hysteresis in single and polycrystalline iron thin films: major and minor loops, first order reversal curves, and Preisach modeling *J. Magn. Magn. Mater.* **395** 361–75